SDMT-based Site Characterization and Liquefaction Analysis of Canal Levees Damaged by the 2012 Emilia (Italy) Seismic Sequence

Laura Tonni
University of Bologna, Italy. E-mail: laura.tonni@unibo.it

Guido Gottardi
University of Bologna, Italy. E-mail: guido.gottardi2@unibo.it

Michela Marchi
University of Bologna, Italy. E-mail: michela.marchi@unibo.it

Luca Martelli
Regione Emilia-Romagna, Servizio Geologico, Sismico e dei Suoli, Bologna, Italy. E-mail: LMartelli@regione.emilia-romagna.it

Paola Monaco
University of L'Aquila, Italy. E-mail: paola.monaco@univaq.it

Lucia Simeoni
University of L'Aquila, Italy. E-mail: lucia.simeoni@univaq.it

Sara Amoroso
Istituto Nazionale di Geofisica e Vulcanologia, L'Aquila, Italy. E-mail: sara.amoroso@ingv.it

Keywords: seismic dilatometer, liquefaction, embankment, Emilia 2012 earthquake

ABSTRACT: The results presented in this paper were obtained as part of a comprehensive study aimed at investigating the post-earthquake stability conditions of canal levees damaged by the May 2012 Emilia (Italy) seismic sequence. This paper is focused on the use of the seismic dilatometer test (SDMT) in the context of the study. In particular the following issues are discussed: (1) Use of SDMT results for soil type identification and ground property characterization of the embankment and the foundation soils; (2) Liquefaction analyses by simplified methods based on the shear wave velocity V_S and on the horizontal stress index K_D provided by SDMT. The results obtained by these methods, in particular those based on K_D, in agreement with results obtained from CPTU interpretation and from laboratory cyclic testing, suggest that local liquefaction phenomena may have been induced by the earthquake in the sandy-silty soils below the canal levee.

1 INTRODUCTION

The seismic sequence which in May 2012 struck a vast area of the Po river plain (Emilia-Romagna region, Northern Italy) caused extensive damage to a number of riverbanks in the epicentral area, in the form of ground deformations, surface fractures and lateral spreading. Major damage was observed in a 3 km long segment of the embankment containing an irrigation canal known as "Canale Diversivo di Burana" near Scortichino, Bondeno (Ferrara), hosting more than one hundred houses and productive activities. In some cases buildings and facilities built on the bank crown were found unstable / unsafe and declared unfit for use.

The municipality of Bondeno, supported by the Emilia-Romagna regional authority in cooperation with the Italian Geotechnical Society (AGI), promoted a Working Group composed of researchers from various Italian universities and experts of the Geological, Seismic and Soil Survey Regional Department, committed to analyzing the seismic response of the embankment, investigating the causes of the earthquake-induced damage, assessing the post-earthquake stability conditions and finally proposing remedial measures. A comprehensive site investigation program, including several in situ and laboratory tests, was performed for this task. The most significant results achieved by the Working Group activity were summarized by

Gottardi et al. (2014) and Tonni et al. (2015). This paper is focused on the use of the results obtained by seismic dilatometer tests (SDMT) in the context of the study.

2 SDMT TESTS IN THE SCORTICHINO EMBANKMENT AREA

2.1 *Testing program and location*

The canal levee and the foundation soils were extensively investigated by in situ tests (5 boreholes, 12 piezocone tests CPTU, 4 seismic dilatometer tests SDMT, piezometer measurements, permeability tests) and by a large number of laboratory tests (triaxial, shearbox, resonant column and cyclic torsional shear, cyclic simple shear, double specimen direct simple shear) on undisturbed and reconstituted samples. Details on the test results and the relevant geotechnical parameters can be found in Gottardi et al. (2014) and Tonni et al. (2015). The site investigations were concentrated along cross-sections in four distinct areas (A, B, C, D, Fig. 1), located at about 1 km distance from each other, in which major concentration of damage had been observed, particularly in the area C. Four SDMT soundings were carried out, one in each investigated area (Fig. 2). In particular, soundings SDMT A, SDMT B and SDMT C were executed from the crest of the embankment, at an elevation of the ground surface between 15.63 m and 17.30 m a.s.l. and pushed to 32-35 m depth, while SDMT D, 25 m deep, was carried out at the toe of the embankment, at an elevation of the ground surface of 9.72 m a.s.l..

2.2 *SDMT results*

Fig. 3 shows the results obtained from all SDMT soundings, referred to the absolute elevation of the ground surface, in terms of profiles with depth of various parameters provided by usual DMT interpretation (Marchetti 1980, Marchetti et al. 2001), i.e. the material index I_D (indicating soil type), the horizontal stress index K_D (related to stress history/OCR), the constrained modulus M, the undrained shear strength c_u (in clay), the friction angle φ' (in sand), as well as the profiles of the measured shear wave velocity V_S and the small strain shear modulus G_0 obtained as $G_0 = \rho V_S^2$.

The SDMT profiles allow recognizing the same stratigraphic sequence and soil units identified by the nearest borehole logs and CPTU results (Gottardi et al. 2014, Tonni et al. 2015). In particular in soundings SDMT A, SDMT B and SDMT C, executed from the crest of the embankment, the material index I_D identified an upper soil layer, about 9-10 m thick, composed of sandy silts and silty sands, corresponding to the core of the man-made embankment (Unit AR) in the topmost 6-7 m and to natural soils (Unit B) in the bottom portion. Unit B is followed by a clayey-silt layer with inclusions of peat and organic material (Unit C), generally about 1-2 m thick, and then by medium to coarse or very coarse sands (Unit A) extending down to the maximum investigated depth, at least 40 m in thickness. In SDMT A and SDMT C thin clayey lenses were identified within Unit A at depths between 30 and 34 m from the crest of the levee. The above schematic soil sequence was encountered in all the investigated areas, with minor variations in thickness of distinct soil units and/or in composition (predominantly sandy or silty) of Units AR and B.

The profiles of SDMT A, SDMT B and SDMT C (Fig. 3) denote rather poor mechanical properties of the soils in the upper ≈ 12 m below the crest of the

Fig. 1. Aerial view of the damaged bank stretch and location of the investigated areas.

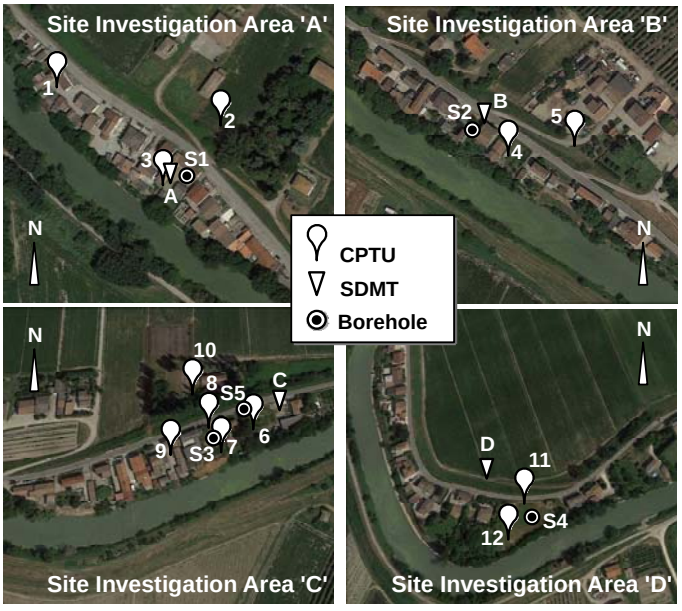

Fig. 2. Location of SDMT and other in situ tests in the four selected areas.

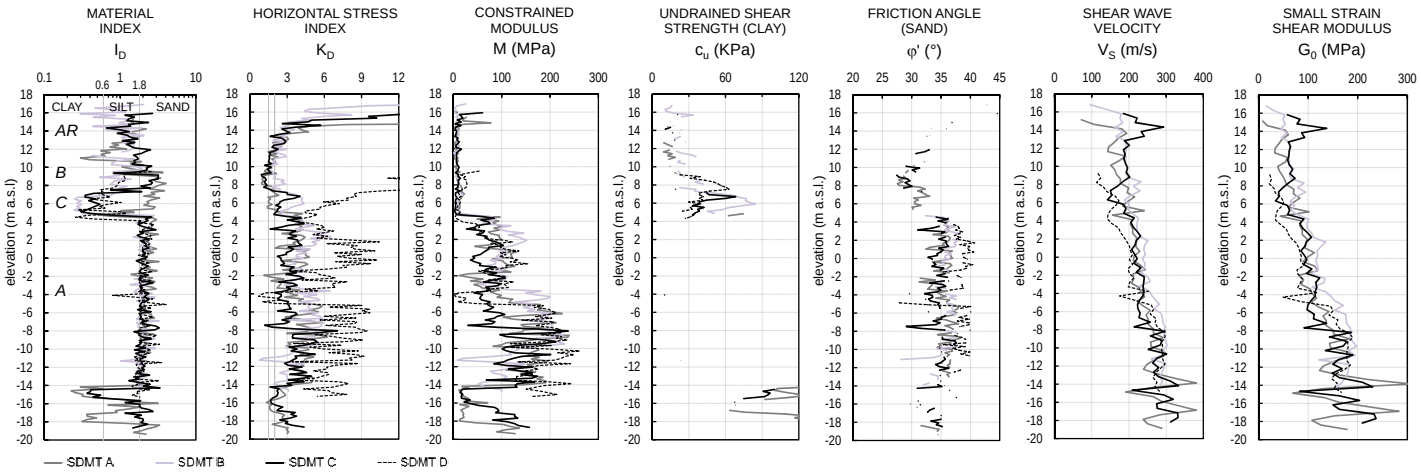

Fig. 3. Superimposed SDMT profiles and identification of distinct soil units.

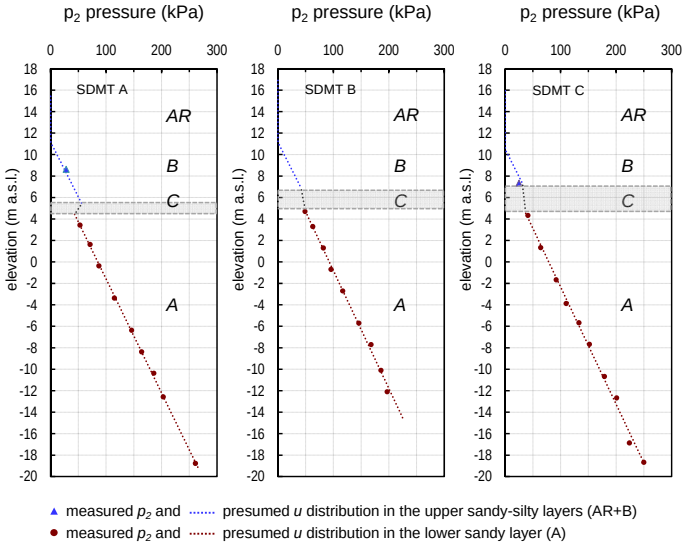

Fig. 4. Profiles of the p_2 pressure measured in sandy-silty layers in SDMT A, SDMT B, SDMT C and pore water pressure distributions inferred from p_2.

embankment (Units AR, B and C). In particular the sandy-silty sediments of Unit B are characterized by low values of the horizontal stress index ($K_D \approx$ 1-2), which imply a low relative density D_R. Only the topmost portion of the embankment (Unit AR), about 2-3 m thick, shows higher K_D values, presumably due to overconsolidation caused by desiccation-wetting cycles.

The sands of Unit A, apart from sporadic thin layers having lower K_D, generally exhibit $K_D \approx$ 3-5, thus denoting a medium relative density (D_R is generally around 60%, according to the correlation D_R-K_D by Reyna & Chameau 1991).

The interpretation of DMT results in the clay layers, excluding the shallow "crusts", indicates that the deposits are normally consolidated or slightly overconsolidated. The coefficient of earth pressure at rest K_0 in the fine-grained layers (silty layers in Units AR, B, C and deep clay layers interbedded in Unit A) is generally $K_0 \approx$ 0.6-0.7.

Differently from the other three soundings, SDMT D was carried out near the toe of the embankment, in the natural soil. It can be presumed that the in situ stress state at this location is far from the K_0 condition. The much higher K_D values observed in SDMT D may then reflect high in situ horizontal stresses near the bank loading area (or also, possibly, higher overconsolidation, since these soils have not been reloaded by the embankment).

Fig. 3 shows that the profiles of V_S measured by SDMTs executed from the top of the embankment in different areas (SDMT A, SDMT B, SDMT C) are very similar. V_S increases gradually with depth from $\approx$ 150-200 m/s in the topmost soil layers to $\approx$ 300 m/s at the maximum investigated depth (32-35 m from the crest). The V_S measured in the upper meters of SDMT D, performed at the toe of the embankment, are lower than the V_S measured in SDMT A, SDMT B, SDMT C at the same absolute elevation, due to the lower overburden stress.

The profiles of the constrained modulus M, obtained by usual DMT interpretation (Marchetti 1980), indicate high compressibility of Units AR, B and C ($M \approx$ 5-10 MPa) and of the deep clay layers, while the sands of Unit A are significantly less compressible. Differently from M, which refers to a "working strain" level (Marchetti et al. 2008), the values of the small strain shear modulus G_0, obtained from V_S measured in the same SDMT sounding, gradually increase with depth, without sharp constrasts between different soil layers.

2.3 *Pore water pressure distribution*

The DMT/SDMT, though not equipped with sensors for measuring the pore pressure, permits to estimate the in situ equilibrium pore water pressure u_0 in high-permeability soils. In fact, experience has

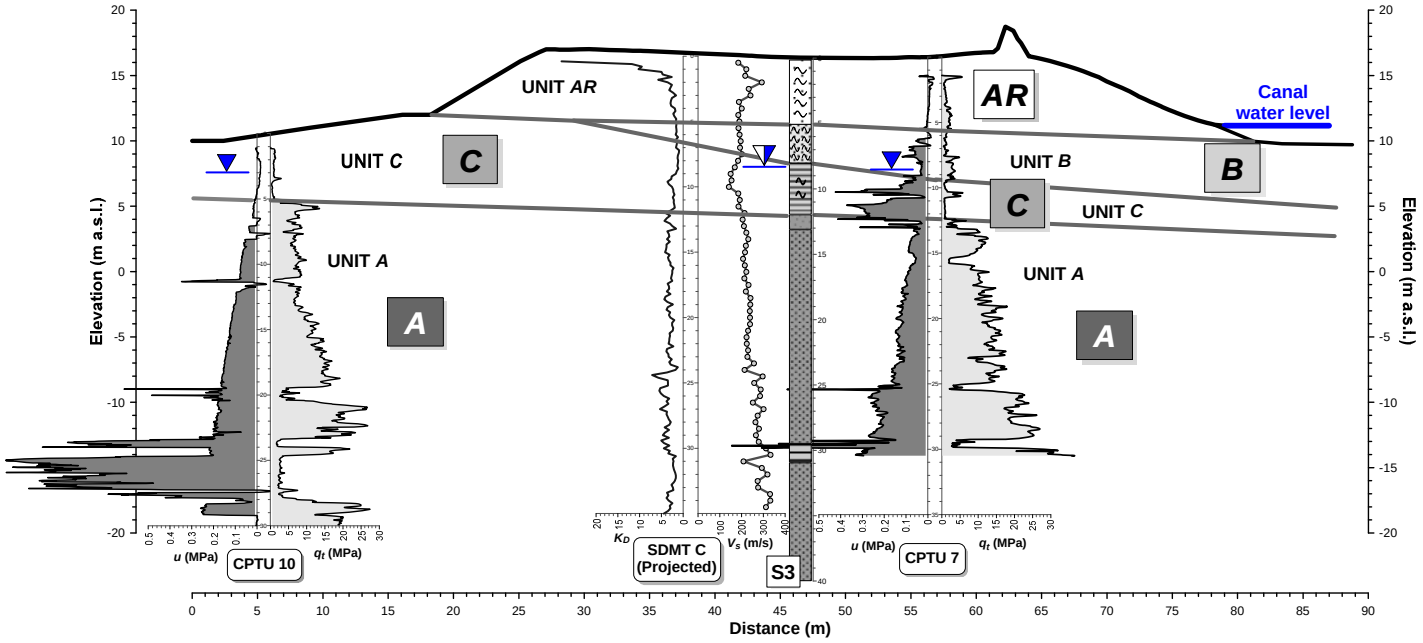

Fig. 5. Stratigraphic model along the cross-section c-c′, area C (Tonni et al. 2015).

shown that, in sands, the pressure p_2 (corrected *C* reading or "closing pressure" measured during depressurization of the membrane) is very close to u_0 (see Marchetti et al. 2001 for details).

At Scortichino p_2 readings were taken at regular depth intervals in the sands of Unit A in all SDMT soundings, while only two p_2 readings were taken in the upper sandy-silty layers (Unit B), one in SDMT A and one in SDMT C. The pore water pressure distributions reconstructed based on p_2 readings (Fig. 4) were used in the interpretation of SDMT results. Interestingly, the interpolation of the p_2 values measured in SDMT A and SDMT C indicates the presence of two distinct groundwater levels: an upper level, located within the embankment core (Unit AR) and the underlying sandy-silty layer (Unit B), generally at 4-5 m depth from the crest, and a lower level within the sandy layer of Unit A ("acquifero padano"), at about 7-8 m depth from the crest, separated by the upper level by an interposed low permeability clay layer (Unit C). This hypothesis was confirmed by measurements in open standpipe piezometers and in nearby existing wells.

The pore water pressure distribution in Unit B was assumed as hydrostatic, presuming that the groundwater level within the embankment core is coincident with the water level in the nearby canal (nearly constant). In Unit A the values of p_2 increase with depth with a gradient slightly lower than the unit weight of water, indicating a non-hydrostatic pore water pressure distribution, compatible with downwards seepage. In Unit C (shaded layer in Fig. 4) the *u* distribution was defined by interpolating the *u* profiles reconstructed in Units B and A.

Based on the above reconstruction, in agreement with piezometer measurements and available information on the water level in the canal, in the liquefaction analyses the groundwater levels and pore water pressure distributions were assumed as follows:

– Embankment (Unit AR) and silty sands-sandy silts (Unit B): groundwater level coincident with the water level in the canal = 11.16 m a.s.l.
– Sands (Unit A): groundwater level = 7.8 m a.s.l.
– Intermediate clay layer (Unit C): *u* values interpolated between (B) and (A)

2.4 *Geotechnical model*

The results of all site investigations were used to construct the geotechnical model of the embankment and the foundation soils in each investigated area. As an example, Fig. 5 (Tonni et al. 2015) shows the geotechnical model defined for the area C (cross-section c-c'), including a borehole log, the profiles of the corrected tip resistance q_t and the pore pressure *u* measured by CPTUs, as well as the profiles of K_D and V_S measured by SDMT.

3 SDMT-BASED LIQUEFACTION ANALYSES

3.1 *Procedure and input data*

In order to identify possible mechanisms responsible of the deformations and fractures observed on the crest of the embankment after the May 20, 2012 earthquake, liquefaction analyses were carried out in each investigated area. The analyses were executed

using a simplified dynamic approach, based on the comparison, at any given depth, of the seismic demand on a soil layer generated by the earthquake (cyclic stress ratio *CSR*) and the capacity of the soil to resist liquefaction (cyclic resistance ratio *CRR*). When *CSR* is greater than *CRR* liquefaction may occur.

CSR was determined by 1-D ground seismic response analyses carried out using the code EERA (Bardet et al. 2000) in terms of total stresses, without taking into account the excess pore pressure build up typical of the liquefaction phenomenon. Details on the input data and results, obtained as part of the Working Group activity, can be found in Gottardi et al. (2014) and Tonni et al. (2015). The earthquake assumed as possible trigger of liquefaction was the May 20, 2012 main shock, recorded at 04:03 (local time), having local magnitude M_L = 5.9 and epicentral distance R_{epi} = 7.5 km from the Scortichino site. The main shock was followed, in about four minutes, by three aftershocks of M_L = 4.8, 4.8 and 5.0 respectively and by nine shocks having M_L > 4 within one hour. Since no ground motion recordings of this event were available in the area of Scortichino, the ground response analyses were carried out using four input accelerograms selected from the Italian earthquake database (ITACA 2011) by use of various search criteria (station on bedrock, M_w = 5.5-6.5, R_{epi} =5-10 km). In addition, a near-fault accelerogram obtained for the April 6, 2009 L'Aquila 2009 earthquake was also considered. All the input accelerograms were scaled to a peak ground acceleration *PGA* = 0.183 *g*, estimated using the attenuation law proposed by Bindi et al. (2011).

At each depth *CSR* was evaluated as:

$$CSR = \frac{\tau_{av}}{\sigma'_{v0}} = \frac{0.65\tau_{\max}}{\sigma'_{v0}} \quad (1)$$

where τ_{max} is the maximum shear stress calculated by ground seismic response analysis (average of τ_{max} calculated using different accelerograms), τ_{av} = 0.65 τ_{max} is the amplitude of the shear stress of the equivalent regular sequence, and σ'_{v0} is the effective overburden stress at the given depth.

CSR was then compared with the cyclic resistance ratio *CRR* estimated by use of various methods based on the SDMT parameters V_S and K_D (described in this paper), on the cone resistance q_t from CPTU and from laboratory cyclic simple shear tests (described in Gottardi et al. 2014 and Tonni et al. 2015).

The liquefaction safety factor FS_{liq} at each depth was calculated as:

$$FS_{liq} = \frac{CRR}{CSR} = \frac{CRR_{M=7.5} \cdot MSF}{CSR} \quad (2)$$

where $CRR_{M=7.5}$ is the cyclic resistance ratio for a reference magnitude M_w = 7.5 (conventionally adopted in the simplified procedure) and *MSF* is a magnitude scaling factor, introduced to account for different magnitudes.

The analysis was carried out considering a magnitude M_w = 6.14, equal to the maximum value expected for a return period of 475 years in the seismogenetic zone in which Scortichino is located and similar to the magnitude of the May 20, 2012 main shock.

The "integral" liquefaction susceptibility at each test location was evaluated by means of the liquefaction potential index I_L (Iwasaki et al. 1982):

$$I_L = \int_{z=0}^{z_{crit}=20m} F(z) \cdot w(z) dz \quad (3)$$

where *w(z)* is a depth weighting factor and the function *F(z)* depends on the safety factor, according to Sonmez (2003).

3.2 *Evaluation of CRR from V_S and K_D by SDMT*

The SDMT permits to obtain two parallel independent estimates of *CRR*, one from the shear wave velocity V_S (measured) and the other from the horizontal stress index K_D (obtained from usual DMT interpretation).

$CRR_{M=7.5}$ was estimated from the overburden stress-corrected shear wave velocity (V_{S1}) using the correlations proposed by Andrus & Stokoe (2000) and Kayen et al. (2013), for different values of the fines content (*FC*). Based on laboratory grain size distribution curves (Gottardi et al. 2014, Tonni et al. 2015), *FC* was assumed > 35% in the sandy-silty layers of Units AR and B, while the sands of Unit A were considered as clean sands ($FC \leq 5\%$).

$CRR_{M=7.5}$ was estimated from K_D using the correlations proposed by Monaco et al. (2005), Tsai et al. (2009) and Robertson (2012), valid for clean sands, without any correction for *FC*. Hence the values of *CRR* estimated from K_D in the sandy-silty layers (Units AR and B) are probably somewhat underestimated (though the low plasticity of fines in these layers should not involve a substantial increase in *CRR*), while in the clean sands of Unit A the *CRR* estimated from K_D are presumably correct.

3.3 *Results and comments*

The results of the liquefaction analyses based on the results of SDMT A, SDMT B and SDMT C (all performed across the embankment) are summarized in Figs 6, 7 and 8, which show, for each sounding,

the profiles with depth of: (1) the material index I_D; (2) the parameter used in each case for evaluating *CRR*, V_{S1} (a) or K_D (b); (3) *CSR* compared to *CRR*; (4) the liquefaction safety factor FS_{liq}; and (5) the liquefaction potential index I_L.

The analyses based on K_D indicated possible occurrence of liquefaction in the silty-sandy soils at the base of the embankment (Unit B), at local depths from the crest between about 5 to 10 m, while no significant liquefaction was detected in the deep sands (Unit A). The liquefaction potential index I_L estimated from K_D by use of different methods, which in Unit B provided similar values of the safety factor FS_{liq}, was found "high" (SDMT A, SDMT C) to "moderate" (SDMT B). On the other hand, the analyses based on V_S generally indicated no or minor liquefaction ("low" I_L). Hence, in the case of Scortichino, *CRR* estimated from V_S appears "less conservative" than *CRR* from K_D.

The results of the liquefaction analyses based on SDMT were compared with the results obtained from CPTU at the same locations (Gottardi et al. 2014, Tonni et al. 2015). As an example, Fig. 9 shows the results obtained based on data from four CPTU tests located in the area C, according to Idriss & Boulanger (2004). The analyses based on CPTU signaled the presence of several liquefiable layers (FS_{liq} < 1) within the silty sand of Unit B, in agreement with the analyses based on K_D. However the liquefaction potential index I_L was found "moderate", i.e. lower than indicated by K_D. A similar trend was observed in all the investigated sections. Fig. 9 also shows the value of FS_{liq} obtained by a laboratory cyclic simple shear test *(CSS)* performed on a silty-sandy sample taken in borehole S3 at 9.70-10.40 m depth. This result (FS_{liq} = 1) confirmed the possible occurrence of liquefaction in the silty-sandy layer.

4 CONCLUSIONS

The results of liquefaction analyses carried out using simplified methods based on the horizontal stress index K_D (SDMT), in agreement with well-established methods based on the cone penetration resistance q_t (CPTU) and laboratory test results, suggest that plausibly local liquefaction phenomena, of variable extent, may have been induced by the May 20, 2012 earthquake in the sandy-silty soils below the Scortichino canal levee. Instead, methods based on the shear wave velocity V_S (SDMT) indicate no or minor liquefaction.

Liquefaction phenomena may have originated

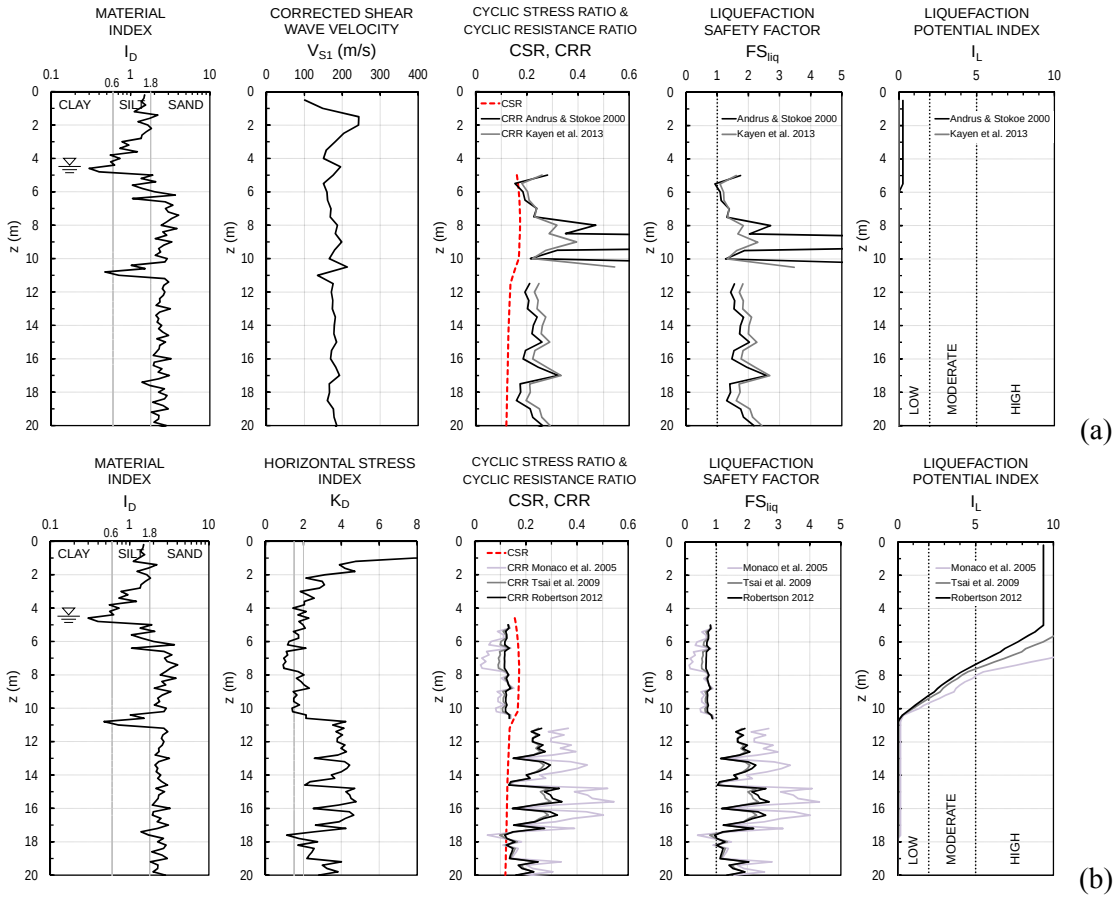

Fig. 6. SDMT A. Results of liquefaction analysis based on: (a) shear wave velocity V_S, (b) horizontal stress index K_D.

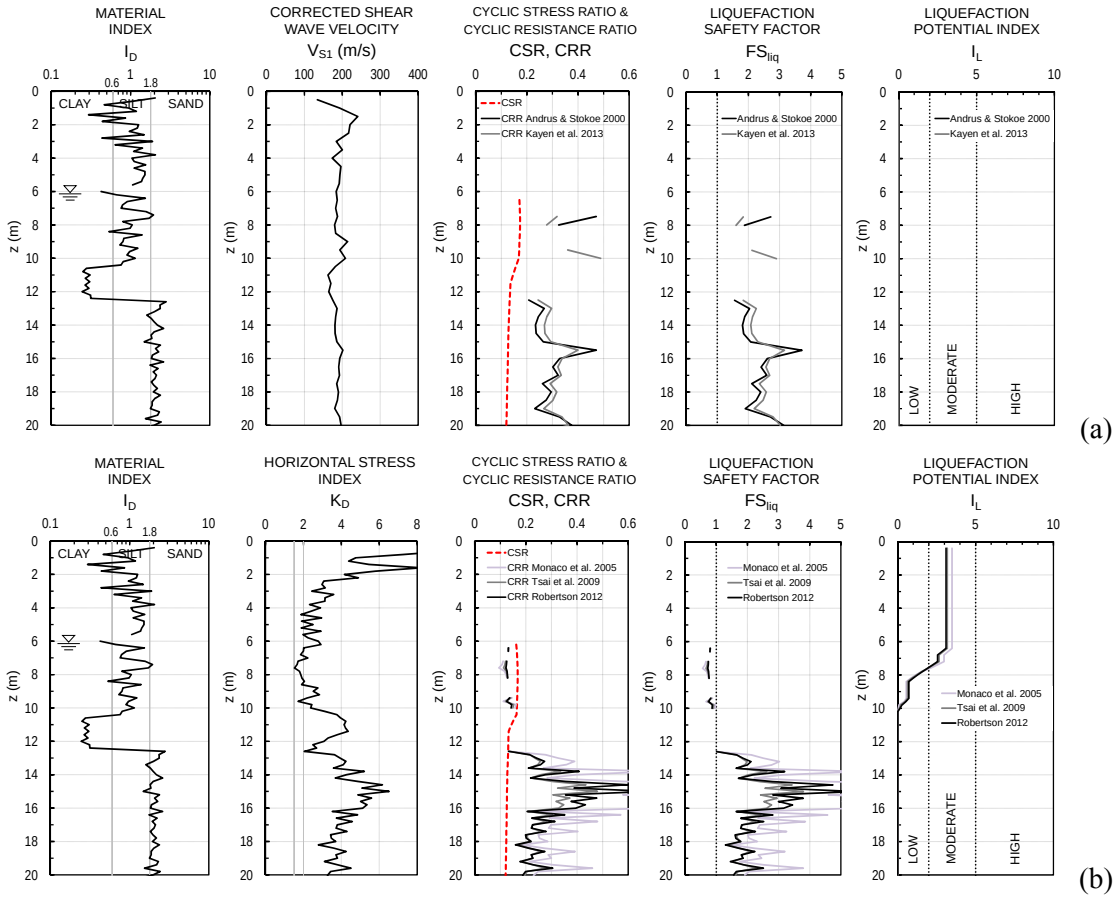

Fig. 7. SDMT B. Results of liquefaction analysis based on: (a) shear wave velocity V_S, (b) horizontal stress index K_D.

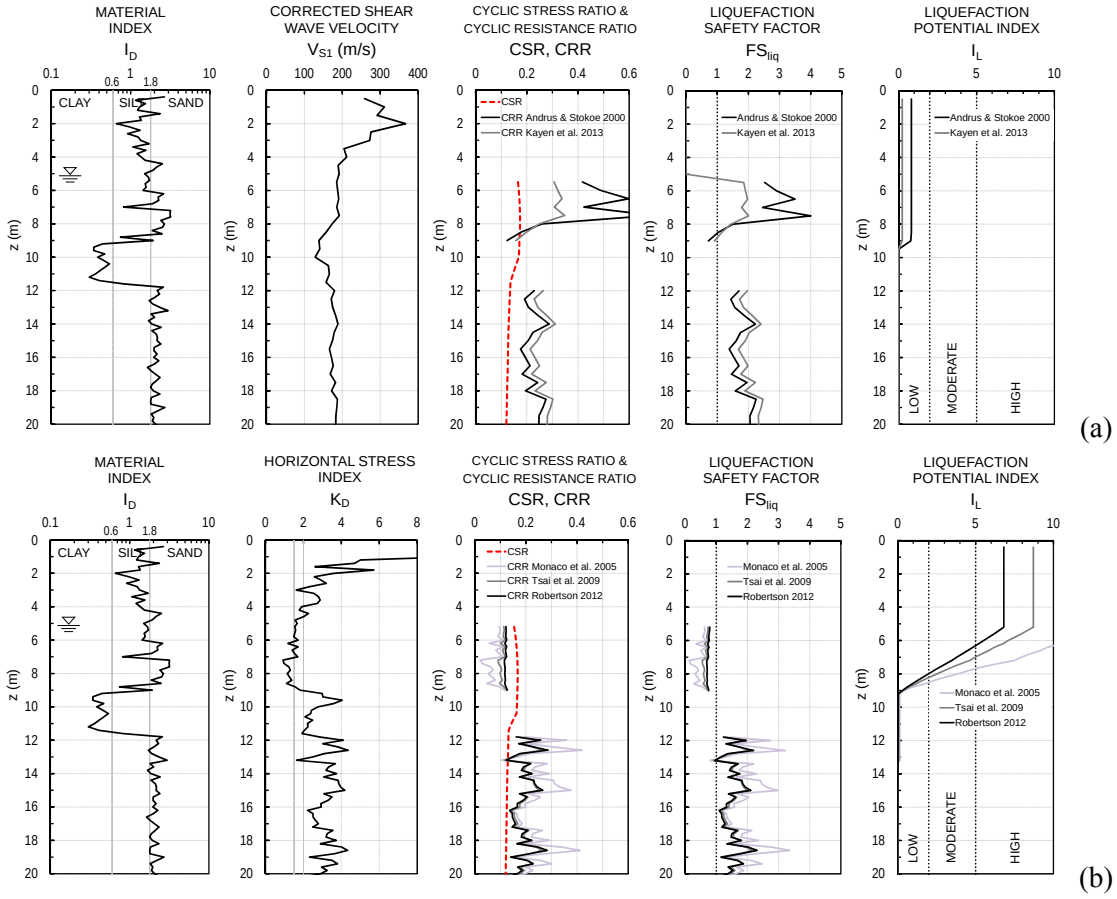

Fig. 8. SDMT C. Results of liquefaction analysis based on: (a) shear wave velocity V_S, (b) horizontal stress index K_D.

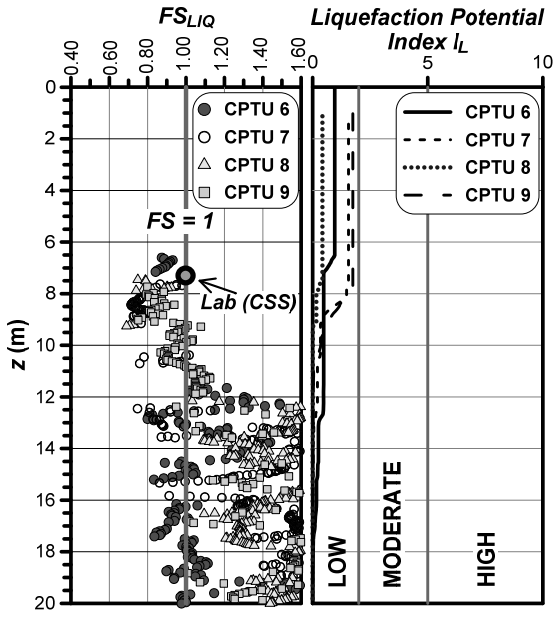

Fig. 9. Area C (cross-section c-c'). Results of liquefaction analyses based on CPTU.

lateral spreading and ground surface deformations observed along the levee crest soon after the earthquake. The presence of groundwater in the embankment core, due to hydraulic connection with the nearby canal, may have played an important role in triggering liquefaction. Moreover the occurrence of several strong aftershocks in a short time span may have caused an accumulation of excess pore pressures, involving a much more severe condition than the single event considered (Sinatra 2013) or corresponding to a single event of greater "equivalent" magnitude (Facciorusso et al. 2014).

5 REFERENCES

Andrus, R.D. and Stokoe, K.H., II. (2000) "Liquefaction resistance of soils from shear-wave velocity." *J. Geotech. Geoenviron. Eng.*, 126(11), 1015-1025.

Bardet, J.P., Ichii, K. and Lin, C.H. (2000) "EERA – A computer program for equivalent-linear earthquake site response analyses of layered soil deposits." Univ. of Southern California.

Bindi, D., Pacor, F., Luzi, L., Puglia, R., Massa, M., Ameri, G. and Paolucci, R. (2011) "Ground motion prediction equations derived from the Italian strong motion database." *Bull. Earthquake Eng.*, 9(6), 1899-1920.

Facciorusso, J., Madiai, C. and Vannucchi G. (2014) "Effetti di liquefazione osservati a San Carlo (FE) durante il terremoto del 20 Maggio e stima del rischio di liquefazione." *Atti XXV Convegno Nazionale di Geotecnica*, Baveno, Italy, 2, 157-164 (in Italian).

Gottardi, G., Amoroso, S., Bardotti, R., Bonzi, L., Chiaradonna, A., d'Onofrio, A., Fioravante, V., Ghinelli, A., Giretti, D., Lanzo, G., Madiai, C., Marchi, M., Martelli, L., Monaco, P., Porcino, D., Razzano, R., Rosselli, S., Severi, P., Silvestri, F., Simeoni, L., Tonni, L. and Vannucchi, G. (2014) "Analisi di stabilità di un argine danneggiato dalla sequenza sismica emiliana del 2012." *Atti XXV Convegno Nazionale di Geotecnica*, Baveno, Italy, 2, 165-175 (in Italian).

Idriss, I.M. and Boulanger, R.W. (2004) "Semi-empirical procedures for evaluating liquefaction potential during earthquakes." *Proc. 11th Int. Conf. on Soil Dyn. and Earthquake Eng. & 33rd Int. Conf. on Earthquake Geotech. Eng.*, Univ. of California, Berkeley, 1, 32-56.

ITACA (2011) ITalian ACcelerometric Archive (1972-2013), version 2.0, http://itaca.mi.ingv.it/ItacaNet/

Iwasaki, T., Tokida, K., Tatsuoka, F., Yasuda, S. and Sato, H. (1982) "Microzonation for soil liquefaction potential using simplified methods." *Proc. 3rd Int. Conf. on Microzonation*, Seattle, 3, 1319-1330.

Kayen, R., Moss, R.E.S., Thompson, E.M., Seed, R.B., Cetin, K.O., Der Kiureghian, A., Tanaka, Y. and Tokimatsu, K. (2013) "Shear-Wave Velocity-Based Probabilistic and Deterministic Assessment of Seismic Soil Liquefaction Potential." *J. Geotech. Geoenviron. Eng.*, 139(3), 407-419.

Marchetti, S. (1980) "In Situ Tests by Flat Dilatometer." *J. Geotech. Eng. Div.*, 106(GT3), 299-321.

Marchetti, S., Monaco, P., Totani, G. and Calabrese, M. (2001) "The Flat Dilatometer Test (DMT) in Soil Investigations – A Report by the ISSMGE Committee TC16." Official version approved by TC16 reprinted in *Flat Dilatometer Testing*, *Proc. 2nd Int. Conf. on the Flat Dilatometer*, Washington D.C., 2006, Failmezger R.A. and Anderson J.B. (eds), 7-48.

Marchetti, S., Monaco, P., Totani, G. and Marchetti, D. (2008) "In Situ Tests by Seismic Dilatometer (SDMT)." *From Research to Practice in Geotechnical Engineering*, *Geotech. Spec. Publ. No. 180*, ASCE, 292-311.

Monaco, P., Marchetti, S., Totani, G. and Calabrese, M. (2005) "Sand liquefiability assessment by Flat Dilatometer Test (DMT)." *Proc. XVI ICSMGE*, Osaka, 4, 2693-2697.

Robertson, P.K. (2012) "The James K. Mitchell Lecture: Interpretation of in-situ tests – some insights." *Proc. 4th Int. Conf. on Geotechnical and Geophysical Site Characterization*, Porto de Galinhas, Brazil, 1, 3-24.

Sinatra, L. (2013) "Simplified procedures and numerical analyses of liquefaction phenomena caused by the Emilia 2012 seismic sequence." Master's degree thesis, Politecnico di Torino.

Sonmez, H. (2003) "Modification of the liquefaction potential index and liquefaction susceptibility mapping for a liquefaction-prone area (Inegol-Turkey)." *Environmental Geology*, 44, 862-871.

Tonni, L., Gottardi, G., Amoroso, S., Bardotti, R., Bonzi, L., Chiaradonna, A., d'Onofrio, A., Fioravante, V., Ghinelli, A., Giretti, D., Lanzo, G., Madiai, C., Marchi, M., Martelli, L., Monaco, P., Porcino, D., Razzano, R., Rosselli, S., Severi, P., Silvestri, F., Simeoni, L., Vannucchi, G. and Aversa, S. (2015). "Analisi dei fenomeni deformativi indotti dalla sequenza sismica emiliana del 2012 su un tratto di argine del Canale Diversivo di Burana (FE)." *Rivista Italiana di Geotecnica* (accepted, in Italian).

Tsai, P., Lee, D., Kung, G.T. and Juang, C.H. (2009) "Simplified DMT-based methods for evaluating liquefaction resistance of soils." *Engineering Geology*, 103, 13-22.